Metastable Superconducting Qubit

Andrew J. Kerman
Lincoln Laboratory, Massachusetts Institute of Technology, Lexington, Massachusetts, 02420, USA
(Received 28 September 2009; published 11 January 2010)

We propose a superconducting qubit design, based on a tunable rf SQUID and nanowire kinetic inductors, which has a dramatically reduced transverse electromagnetic coupling to its environment, so that its excited state should be metastable. If electromagnetic interactions are in fact responsible for the current excited-state decay rates of superconducting qubits, this design should result in a qubit lifetime orders of magnitude longer than currently possible. Furthermore, since accurate manipulation and readout of superconducting qubits is currently limited by spontaneous decay, much higher fidelities may be realizable with this design.

DOI: 10.1103/PhysRevLett.104.027002 PACS numbers: 85.25.Cp, 03.67.Lx

One of the distinguishing features of Josephson-junction (JJ)-based qubits is their strong coupling to electromagnetic (EM) fields, which permits fast operations (~1–10 ns for single-qubit gates and 10–100 ns for coupled-qubit gates). However, it may also be responsible for their short excited-state lifetimes ($\lesssim 4\ \mu$s [1–5]); that is, assuming the decay process is electromagnetic, its rate depends on the same matrix element which governs intentional qubit manipulations by external fields. Unfortunately, understanding and controlling spontaneous decay of these circuits has so far proved difficult, because it also depends on their EM environment at GHz frequencies. This environment is affected not only by packaging and control lines, but also by microscopic degrees of freedom in the substrate, surface oxides, and JJ barrier dielectrics. In fact, low-frequency noise due to microscopic fluctuators is already known to produce "dephasing" of qubits [1–5]. Although little is yet certain about the properties of these degrees of freedom, work is ongoing to study them [6] and to reduce their number through improved materials and fabrication [7]. In this Letter, we discuss a different approach, seeking a qubit which is insensitive to high-frequency EM fluctuations *by design*, and which should have a much longer excited-state lifetime with *existing* materials and fabrication techniques. This is a departure from the highly successful computational architecture known as circuit QED [8], in which strong transverse coupling to EM fields is both a prerequisite and a figure of merit.

The decay rate of an excited state $|e\rangle$ to lower-lying state $|g\rangle$ is typically given by Fermi's golden rule: $\Gamma \equiv 1/T_1 = (2\pi/\hbar)|m_i|^2\rho(\hbar\omega_{eg})$, where $m_i \equiv \langle e|\hat{H}_i|g\rangle$, $\hat{H}_i$ is a Hamiltonian describing the coupling between the qubit and a continuum (e.g., the excited states of an ensemble of two-level systems—TLSs), and $\rho(\hbar\omega_{eg})$ is the density of states in that continuum at the energy $\hbar\omega_{eg} \equiv E_e - E_g$. The m_i can be nonzero for a JJ-based qubit when the flux through a loop, the induced charge across a JJ, or a JJ critical current depends on the state of one or more TLSs. To minimize the resulting decay rate, we must reduce ρ or m_i. Our focus here will be on the latter.

A good choice for qubit energy levels which are weakly coupled to each other by EM fields are the flux states of an rf SQUID [Fig. 1(a)] [9] at large E_J/E_C, where $E_J = \Phi_0 I_C/2\pi$ and $E_C \equiv e^2/2C_{\rm tot}$ are the Josephson and charging energies (I_C is the JJ critical current, $\Phi_0 \equiv h/2e$, and $C_{\rm tot}$ is the total capacitance across the JJ). When $\Phi_{\rm rf} \sim \Phi_0/2$, two quantum states, in which either zero or one fluxon is contained in the loop, become nearly degenerate and are separated by a potential barrier [Fig. 1(b)]. The Hamiltonian for the rf SQUID is [10]

$$\hat{H} = 4E_C(\hat{n} - n_e)^2 - E_J\cos\hat{\phi} + E_L\hat{\gamma}^2/2, \qquad (1)$$

where $\hat{\phi}$ is the phase across the JJ, $\hat{n} \equiv -id/d\phi$ is operator corresponding to the number of Cooper pairs that have tunneled through the JJ, $\hat{\gamma} \equiv \hat{\phi} + 2\pi f$ is the phase across the inductor, $f = \Phi_{\rm rf}/\Phi_0$, and $E_L \equiv (\Phi_0/2\pi)^2/L$. The quantity n_e is a fluctuating offset charge across $C_{\rm tot}$ induced by capacitances to the environment or by tunneling of quasiparticles through the junction (at dc $n_e = 0$ due to the inductive shunt [10]).

We diagonalize $\hat{H}$ on a lattice of γ points to obtain wave functions $\psi_k(\gamma) \equiv \langle\gamma|k\rangle$ [Figs. 1(c), 1(e), and 1(g)], which are then used to evaluate matrix elements $\langle k|\hat{H}_i|k'\rangle$ [11] for flux, charge, and I_C-coupled TLSs with: $\hat{H}_f \equiv 2\pi\delta f E_J\sin(\hat{\gamma} + 2\pi f)$, $\hat{H}_n \equiv 8\delta n E_C\hat{n}$, and $\hat{H}_I \equiv \delta I_C E_J\cos(\hat{\gamma} + 2\pi f)$, respectively; δf, δn, and δI_C are the (small) amplitudes of TLS-state-dependent changes in f, n_e, and I_C. These amplitudes will be different for each TLS, so it is conceptually useful to recast the golden rule in terms of an average noise power spectral density S_i [11], so that: $\Gamma_i \equiv |d_i|^2 S_i(\omega_{eg})/\hbar^2$, where $d_i \equiv \langle e|\hat{X}_i|g\rangle$ are analogous to a transition dipole for each fluctuation, and $\hat{X}_f \equiv 2\pi E_J\sin(\hat{\gamma} + 2\pi f)$, $\hat{X}_n \equiv 8E_C\hat{n}$, $\hat{X}_{I_C} \equiv E_J\cos(\hat{\gamma} + 2\pi f)$ with units of energy per Φ_0, electron pair, and current.

Since the operators $\hat{X}_i$ are local in $\hat{\gamma}$, a way to reduce all of the d_i at once is to reduce the overlap of the probability distributions $|\psi_g(\gamma)|^2$ and $|\psi_e(\gamma)|^2$. This overlap results from tunneling through the barrier [Figs. 1(b) and 1(c)], so to minimize it we detune the left and right

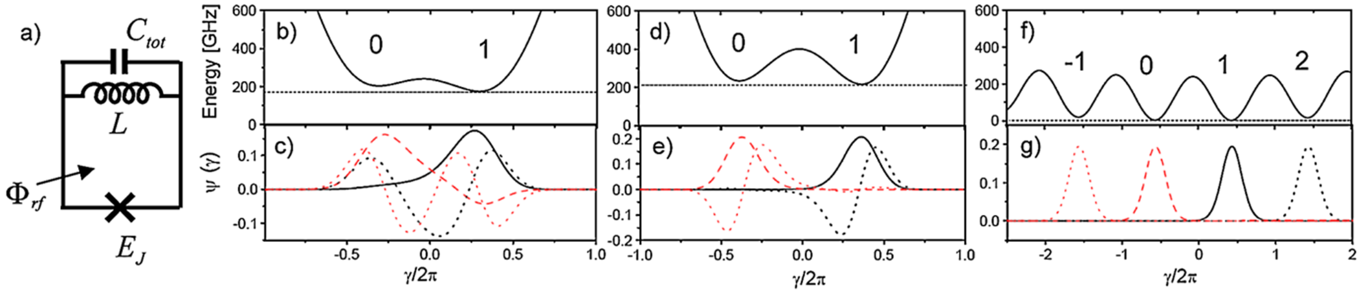

FIG. 1 (color online). Fluxon tunneling for the rf-SQUID flux qubit. (a) Schematic. (b), (d), (f) Potential. (c), (e), (g) Qubit level wave functions $\psi_g(\gamma)$ (solid line) and $\psi_e(\gamma)$ (dashed line) for $f = 0.515$. For (b), (c), E_J, E_C, $E_L = h \times 120, 6, 60$ GHz. For (d), (e), E_J, E_C, $E_L = h \times 180, 4, 60$—the potential barrier between wells is higher so the tunneling is weaker. For (f), (g), E_J, E_C, $E_L = h \times 120, 6, 0.375$. Dotted lines in (c), (e), and (g) show the next excited states. In (c) and (e), these are "vibrational" excitations, while in (g) they are the ground states of adjacent wells (-1 or 2 fluxons in the SQUID loop, as indicated).

wells from each other ($f \neq 0.5$) and increase the barrier height by increasing E_J/E_C and E_J/E_L [Figs. 1(d) and 1(e)].

Unfortunately, when $f \neq 0.5$, $d\omega_{eg}/df \neq 0$, and nonzero, low-frequency δf produce dephasing [1,12]. This sensitivity can be reduced by increasing L, since $\hbar\omega_{eg} \approx \frac{\Phi_0^2}{L}(f - 0.5)$, for $E_L \ll E_J$ [13]. To realize large L, increasing the loop size is not attractive, both because it would need to be of millimeter scale and because its large capacitance would limit E_C. Instead, we propose using the kinetic inductance of a long meandered nanowire patterned from thin ($\sim$5 nm-thick) NbN, which can have sheet inductance as large as $\sim$100 pH and $I_C \sim 20$ μA [14,16]. A 10 μm-square meander of 100-nm-wide wire gives $L \sim 500$ nH [16], and EM simulation shows a shunt capacitance of only $\sim$0.4 fF (compare to $\sim$3.2 fF for the JJs we consider below) [17].

Figure 2(a) shows the $|d_i|$ for our qubit, as a function of E_J/E_C. Also shown are the $|d_i|$ for quantronium [5], transmon [3], flux [1,2], and phase [4] qubits [18]. Based on these results, and by extracting bounds on the S_i from T_1 values observed in Refs. [1–5], we can estimate T_1 for our qubit. Not surprisingly, no single set of S_i, in conjunction with the calculated d_i, can accurately explain all of the observations, since the noise levels are likely somewhat different in each experiment; however, for the present purpose, we take $S_I(5\text{ GHz}) \lesssim 1.4 \times 10^{-17}$ $\mu\text{A}^2\,\text{Hz}^{-1}$ from $T_1 = 650$ ns for the phase qubit of Ref. [4], $S_n(5.7\text{ GHz}) \lesssim 1.6 \times 10^{-15}$ Hz^{-1} from $T_1 = 1.7$ μs for the transmon of Ref. [3], and $S_f(5.5\text{ GHz}) \lesssim 1.3 \times 10^{-20}$ Hz^{-1} from $T_1 = 2$ μs from the flux qubit of Ref. [1]. Figure 2(b) shows the resulting estimate of T_1 for our qubit (dominated by S_n). For $E_J/E_C \sim 3$, $T_1 \sim 3$ μs (roughly consistent with Ref. [15]); however, at $E_J/E_C = 20$, $T_1 \sim 950$ ms.

The reduced transverse coupling that we achieve through increasing E_J/E_C and E_J/E_L also means we must drive the qubit with larger fields to manipulate it. If the required driving becomes too strong, spurious effects can occur such as off-resonant excitation to short-lived excited states (followed by decay). Furthermore, initializing the qubit will take longer as the T_1 is increased. We therefore want to be able to adjust E_J/E_C in real time using a tunable rf SQUID [Fig. 2(c)] (analogous to the tunable flux qubit [19,20]). The single JJ is replaced by a dc SQUID, and the rf SQUID loop is replaced with a gradiometric design where $f_{\rm rf} \equiv (\Phi_1 - \Phi_2)/\Phi_0$ [20]. In this configuration, E_J in Eq. (1) is replaced with:

$$E_J(f_{\rm dc}) = 2E_{J0}\cos[\pi f_{\rm dc} - \hat{\gamma}_{\rm dc}/2] \approx 2E'_{J0}\cos[\pi f_{\rm dc}], \quad (2)$$

where E_{J0} is the Josephson energy of each JJ, $f_{\rm dc} = \Phi_{\rm dc}/\Phi_0$, and $\hat{\gamma}_{\rm dc}$ is the phase across $L_{\rm dc}$, the self-inductance of the dc-SQUID loop. To obtain the right-hand side of Eq. (2), we note that for $L_{\rm dc} \ll L$, $L_J \equiv \Phi_0/2\pi I_C$, the zero-point fluctuations of $\hat{\gamma}_{\rm dc}$ can be adiabatically eliminated, yielding only a small renormalization of E_{J0} [21] (for $L_{\rm dc} < 50$ pH, and the parameters under consideration here, a fraction of a percent).

The qubit can be manipulated (or measured dispersively [22]) with $V_{\rm rf}$, $\Phi_{\rm dc}$, or $\Phi_{\rm rf} \equiv \Phi_1 - \Phi_2$ [Fig. 2(c)]. We

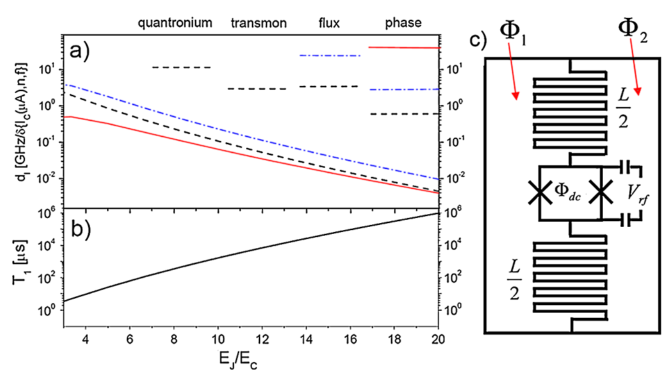

FIG. 2 (color online). Transverse coupling of the metastable rf-SQUID qubit versus E_J/E_C for E_C, $E_L = h \times 6, 0.375$ GHz, and $f = 0.57$. Panel (a) shows $|d_n|$ (dashed line), $|d_f|$ (dash-dotted line), and $|d_{I_C}|$ (solid line), respectively. Horizontal lines show equivalent $|d_i|$ for the quantronium [5], transmon [3], flux [1,2], and phase [4] qubits. Panel (b) shows the estimated T_1 for the metastable rf-SQUID qubit. (c) Schematic. E_J/E_C is tunable through $\Phi_{\rm dc}$.

discuss the first two here. In order to describe large-amplitude driving, and to incorporate spontaneous decay between instantaneous energy eigenstates $|m(t)\rangle'$, we use a time-dependent transformation to the instantaneous energy eigenbasis, yielding the Hamiltonian: $\hat{H}_{ad} = \hat{R}\hat{H}\hat{R}^\dagger - i\hbar\hat{R}\frac{d}{dt}\hat{R}^\dagger$, where $\hat{H}$ is given by Eq. (1) and $\hat{R}$ is defined by $\hat{R}|\psi\rangle \equiv |\psi\rangle'$ [the prime indicates the time-dependent basis $|m(t)\rangle'$]. The first term in $\hat{H}_{ad}$ is diagonal, containing the time-dependent eigenenergies, and the second term yields nonadiabatic transitions between levels. We integrate a master equation based on $\hat{H}_{ad}$, truncated to the 10 lowest-lying instantaneous eigenstates [up to $\gtrsim$100 GHz above $|g\rangle$ and including excited vibrational levels in the four lowest-lying potential wells in Fig. 1(f)] [23]. To this we add a spontaneous decay rate $\Gamma_{mn}(t)$ from each level $|m\rangle'$ to each other level $|n\rangle'(T_1 \equiv 1/\Gamma_{10})$. To generate the $\Gamma_{mn}(t)$, we use Fermi's golden rule and assume an Ohmic noise spectrum $S_i(\omega) \propto \hbar\omega/(1 - e^{-\hbar\omega/k_BT})$ ($\omega > 0$ denotes downward transitions and $\omega < 0$ upward transitions), with the overall amplitude for each type of noise discussed above. The time dependence of the $\Gamma_{mn}(t)$ comes from the $|X_i(t)|^2_{mn}$.

As a test case, we consider a π pulse, where the qubit starts in $|g\rangle$, for which an indication of gate fidelity is how much population we can put in $|e\rangle$, as shown in Fig. 3. We take $E_C, E_L = h \times 6, 0.375$ GHz ($L = 430$ nH) and $f_{\rm rf} = 0.57$ ($\omega_{eg} = 2\pi \times 1.034$ GHz [24]). For modulation of $\Phi_{\rm dc}$ (solid line), we use the pulse shown in the left inset to Fig. 3, which starts and ends at $E_J = h \times 200$ GHz (with $2E'_{J0} = h \times 280$ GHz). For modulation of $V_{\rm rf}$, we take a fixed $E_J = h \times 42$ GHz. The simulation yields $1 - P_e = 1.1 \times 10^{-5}$ and 2.5×10^{-5} for $\Phi_{\rm rf}$ and $V_{\rm rf}$ modulation, respectively. The former is limited almost completely by decay of $|e\rangle$ during the brief excursions to smaller E_J/E_C where $\Gamma_{10}(t)$ is larger. This also explains the shape of the time evolution: the drive becomes effectively faster when E_J/E_C is smaller, producing the upward "steps."

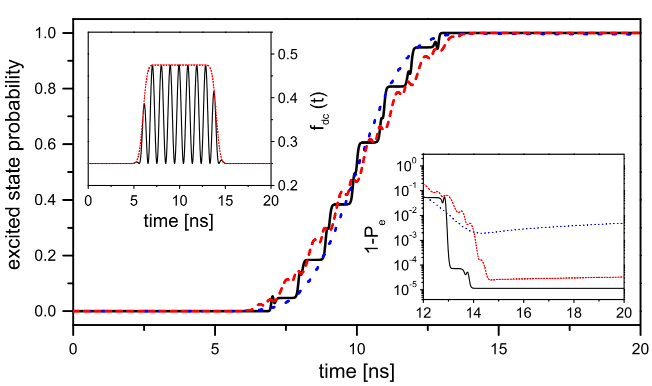

FIG. 3 (color online). Manipulation of the metastable rf-SQUID qubit. Integration of the master equation for the qubit, undergoing a π pulse starting from $|g\rangle$. The solid line is for the modulation of $\Phi_{\rm dc}$ in the left inset; the dashed line is for a sinusoidal modulation of $V_{\rm rf}$. The dotted line is the equivalent result for a flux qubit [1,2].

Spurious excitation to adjacent fluxon states [-1, 2 in Fig. 1(f)] and higher vibrational states are at the $\mathcal{O}(10^{-6})$ level. Driving with $V_{\rm rf}$ is limited by off-resonant excitation of the first vibrational levels (at $\sim$40 GHz) followed by decay. This process is suppressed for $\Phi_{\rm dc}$ modulation since the perturbation is nearly even about the potential well center. For comparison is shown the same simulation for a flux qubit [1,2], which has $1 - P_e = 2 \times 10^{-3}$, due to decay from $|e\rangle$.

This simulation does not include $1/f$ flux noise [1]. To estimate its effect, we use the results of Ref. [25] and the fact that for $L = 430$ nH, $d\omega_{eg}/d\Phi_{\rm rf} = 2\pi \times 14.3$ MHz/mΦ_0 ($\sim$100 times smaller than a typical flux qubit far from $f = 0.5$). For the noise amplitude measured in Ref. [1], we calculate the average error in the qubit relative phase over the 8-ns π pulse to be $\sim$4.5 mrad, which for the maximally sensitive $(|g\rangle + |e\rangle)/\sqrt{2}$ state gives an error probability of only $\sim 2.0 \times 10^{-5}$ [26].

By eliminating the transverse coupling induced by external fields, we have also eliminated the usual mechanism for coupling qubits to each other [27]. Instead, we can use a longitudinal coupling, similar to Refs. [28,29]. A schematic of our proposed circuit is shown in Fig. 4(a). Two rf-SQUID qubits are coupled by mutual inductances M to a third coupler qubit with large persistent current I_p^C, biased at its degeneracy point ($f_{\rm rf}^C = 0.5$). The approximate Hamiltonian is

$$\hat{H} \approx \sum_i^{1,2,C} [\epsilon_i \hat{\sigma}_i^z + \Delta_i \hat{\sigma}_i^x] + J_C \hat{\sigma}_C^z [\hat{\sigma}_1^z + \hat{\sigma}_2^z] + J_0 \hat{\sigma}_1^z \sigma_2^z. \quad (3)$$

Here, eigenstates of $\hat{\sigma}^z$ are persistent current states; $J_C = MI_p^C d\epsilon_{1,2}/d\Phi$, where $d\epsilon_{1,2}/d\Phi \approx 4\pi^2 E_L/\Phi_0$ [28], and $J_0 = M_0 I_{p1} I_{p2}$. We take E_J, $E_C = h \times 200$, 6 GHz, and $L = 430$ nH for the data qubits (yielding $\Delta_{1,2} = h \times 52$ kHz and $I_{p1,2} \approx \Phi_0/2L = 2.4$ nA) and E_J, $E_C = h \times 5000$, 0.7 GHz, and $L = 35$ nH for the coupler (yield-

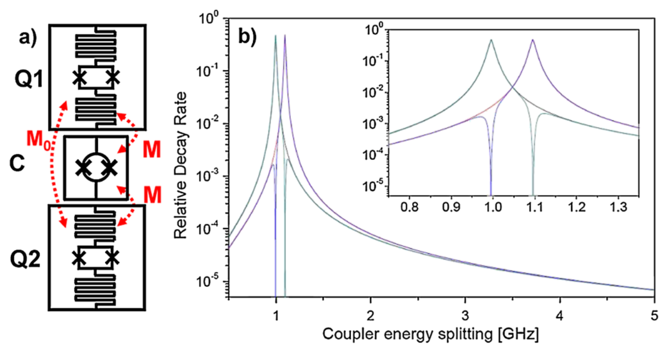

FIG. 4 (color online). Switchable coupling between metastable rf-SQUID qubits. (a) Schematic. Two data qubits are coupled through a mutual inductance M to a coupler qubit. Panel (b) shows the calculated decay rates for the four computational levels, relative to the decay rate of the coupler in isolation, with ϵ_1, $\epsilon_2 = h \times 1.0$, 1.1 GHz (chosen to be different only for clarity). The inset shows the resonances that occur due to nonzero $\Delta_{1,2}$.

ing $I_p^C = 5.2\ \mu$A, $\Delta_C = h \times 5$ GHz). With $M = 5$ pH, $M_0 = 0.1$ pH, we obtain $J_C = h \times 188$ MHz, $J_0 = h \times 0.87$ kHz, giving a conditional frequency shift $h\delta_\nu \approx 2J_C^2/t_C - J_0 = h \times 14.1$ MHz [28] and a conditional-$\pi/2$ gate in 18 ns. If we use spin echoes [25,28], the residual phase drift due to $1/f$ flux noise (not canceled by the echo) during this time is 3.6 mrad, producing a maximal error (in addition to that from the π pulse) of 3.0×10^{-6} [26].

A very small transverse coupling to the data qubits also means that their excited states will undergo negligible mixing with the excited state of the coupler (which will likely be short lived). Figure 4(b) shows the decay rates that result. These are proportional to $|\langle ij|\hat{\sigma}_C^z|kl\rangle|^2$ ($i, j, k, l \in \{g, e\}$), where $|ij\rangle$ are the computational states [the lowest four eigenstates of Eq. (3), which in the $J_C \to 0$ limit correspond to the coupler in its ground state [28]]. The pronounced peaks (and dips) occur when the coupler is nearly resonant with one of the data qubits; in these regions, the nonzero $\Delta_{1,2}$ produce two entangled states of a data qubit and the coupler, with one state coupling maximally to fluctuations and the other minimally. When both qubits are detuned far from the coupler, their decay rate is sufficiently suppressed that even coupler lifetimes at the nanosecond scale would have little effect.

In summary, we have described a qubit design with weak transverse coupling to EM fields. This qubit should be significantly less sensitive to microscopic EM degrees of freedom arising from materials and fabrication imperfections and may permit very long T_1 times with good device yield using present-day materials and fabrication techniques. If the predictions of this Letter are correct, significantly higher gate and measurement fidelities may be possible, pushing JJ-based qubits further towards fault tolerance and scalability.

We acknowledge helpful discussions with William Oliver, Jeremy Sage, and Jens Koch. This work is sponsored by the U.S. Air Force under Contract No. FA8721-05-C-0002. Opinions, interpretations, recommendations, and conclusions are those of the authors and are not necessarily endorsed by the U.S. Government.

[1] F. Yoshihara, K. Harrabi, A. O. Niskanen, Y. Nakamura, and J. S. Tsai, Phys. Rev. Lett. **97**, 167001 (2006).
[2] P. Bertet *et al.*, Phys. Rev. Lett. **95**, 257002 (2005).
[3] J. A. Schreier *et al.*, Phys. Rev. B **77**, 180502(R) (2008).
[4] M. Hofheinz *et al.*, Nature (London) **459**, 546 (2009).
[5] I. Siddiqi *et al.*, Phys. Rev. B **73**, 054510 (2006).
[6] S. Sendelbach, D. Hover, M. Muck, and R. McDermott, Phys. Rev. Lett. **103**, 117001 (2009); Z. Kim *et al.*, Phys. Rev. B **78**, 144506 (2008); S. Sendelbach *et al.*, Phys. Rev. Lett. **100**, 227006 (2008); R. W. Simmonds *et al.*, Phys. Rev. Lett. **93**, 077003 (2004); A. Lupascu, P. Bertet, E. F. C. Driessen, C. J. P. M. Harmans, and J. E. Mooij, arXiv 0810.0590.
[7] J. M. Martinis *et al.*, Phys. Rev. Lett. **95**, 210503 (2005); J. S. Kline, H. Wang, S. Oh, J. M. Martinis, and D. P. Pappas, Supercond. Sci. Technol. **22**, 015004 (2009); S. Oh *et al.*, Phys. Rev. B **74**, 100502(R) (2006).
[8] R. J. Schoelkopf and S. M. Girvin, Nature (London) **451**, 664 (2008), and references therein.
[9] J. R. Friedman, V. Patel, W. Chen, S. K. Tolpygo, and J. E. Lukens, Nature (London) **406**, 43 (2000).
[10] J. Koch, V. Manucharyan, M. H. Devoret, and L. I. Glazman, Phys. Rev. Lett. **103**, 217004 (2009).
[11] J. Q. You, X. Hu, S. Ashhab, and F. Nori, Phys. Rev. B **75**, 140515(R) (2007).
[12] Note that even flux and transmon qubits, for which $d\omega_{eg}/d\Phi$ can be zero, still have $d\omega_{eg}/dI_C \neq 0$, and this may soon become a limitation [D. J. Van Harlingen *et al.*, Phys. Rev. B **70**, 064517 (2004)].
[13] Note that Ref [9] was in the opposite limit $E_J \ll E_L$.
[14] In [15], a series array of JJs was used to create a large inductor for a similar qubit design for the purpose of suppressing charging effects at $E_J/E_C \sim \mathcal{O}(1)$. This method cannot be used at large E_J/E_C to strongly suppress d_i in the manner discussed here, since each of these JJs is a tunneling path for the fluxon. Although fluxons can in principle tunnel through NbN nanowires (due to their granular microstructure), we estimate the rate for this process to be $<\mathcal{O}$ (1 s^{-1}).
[15] V. Manucharyan, J. Koch, L. I. Glazman, and M. H. Devoret, Science **326**, 113 (2009); V. Manucharyan, J. Koch, M. Brink, L. I. Glazman, and M. H. Devoret, arXiv: cond-mat/0910.3039.
[16] A. J. Kerman *et al.*, Appl. Phys. Lett. **88**, 111116 (2006).
[17] In applying Eq. (1) to this structure, we are treating it as a lumped element, implicitly neglecting coupling to its internal modes.
[18] For the transmon and quantronium, $d_{I_C} = d_f = 0$, and for the flux qubit at $f = 0.5$, $d_{I_C} = 0$.
[19] T. P. Orlando *et al.*, Phys. Rev. B **60**, 15 398 (1999).
[20] F. G. Paauw, A. Fedorov, C. J. P. M. Harmans, and J. E. Mooij, Phys. Rev. Lett. **102**, 090501 (2009).
[21] A. M. van den Brink, Phys. Rev. B **71**, 064503 (2005).
[22] Dispersive measurement becomes more difficult as the transverse coupling is reduced. To measure the qubit state at very weak coupling, a dc SQUID coupled to the qubit through kinetic mutual inductance could be used [1].
[23] Including additional levels had no effect, as these levels are not populated by the present manipulations.
[24] A relatively small ω_{eg} is used to minimize off-resonant excitation of the adjacent fluxon states.
[25] G. Ithier *et al.*, Phys. Rev. B **72**, 134519 (2005).
[26] For the present qubit, Eq. (22) of Ref. [25] yields $\Gamma_{\mathrm{echo}} = (13\ \mu\mathrm{s})^{-1}$ for the flux noise measured in Ref. [1].
[27] A. O. Niskanen *et al.*, Science **316**, 723 (2007); T. Hime *et al.*, Science **314**, 1427 (2006); S. H. W. van der Ploeg *et al.*, Phys. Rev. Lett. **98**, 057004 (2007); L. DiCarlo *et al.*, Nature (London) **460**, 240 (2009); S. Ashhab *et al.*, Phys. Rev. B **77**, 014510 (2008).
[28] A. J. Kerman and W. D. Oliver, Phys. Rev. Lett. **101**, 070501 (2008).
[29] Y.-D. Wang, A. Kemp, and K. Semba, Phys. Rev. B **79**, 024502 (2009). Note that in this scheme, the coupling is switched off by tuning the qubits to degeneracy, so it would not be applicable here.